

# Covariant correlation-disturbance and its experimental realization with spin-1/2 particles

Ali Asadian<sup>1</sup>, Florian Gams<sup>2</sup>, and Stephan Sponar<sup>2</sup>

<sup>1</sup>*Department of Physics, Institute for Advanced Studies in Basic Sciences (IASBS), Gava Zang, Zanjan 45137-66731, Iran*

<sup>2</sup>*Atominstytut, TU Wien, Stadionallee 2, 1020 Vienna, Austria*

We formulate a precise tradeoff relation between correlation and disturbance in a sequential quantum measurement setup. This relation, examined for qubit case, highlights key symmetry properties useful for the robust estimation and characterization of measurement parameters in the presence of local unitary noise, or in scenarios lacking shared reference frames. In addition, we report on the experimental implementation of the proposal in a neutron optical experiment, which proved particularly valuable for calibrating and optimizing measurement devices as confirmed by the theoretical result.

*Introduction.*— Incompatibility between measurements is a fundamental aspect of quantum mechanics, leading to distinctive features such as nontrivial uncertainty [1, 2] and complementarity [3] relations. At its core, quantum violations of various classical models—commonly referred to as hidden variable models [4–6]—necessitate this measurement incompatibility, which can be verified solely through observed statistics without relying on specific assumptions about the devices [7]. Identifying scenarios that exhibit the characteristic features of measurement incompatibility and disturbance is now a central objective for both fundamental research and practical applications, as it has been recognized as a key resource underlying many quantum communication tasks that outperform classical methods [8–10]. Understanding and controlling measurement disturbance has far-reaching implications for developing precise and reliable quantum technologies [11–13].

One of the most fundamental approaches to quantum measurement disturbance and uncertainty is investigated via a temporal sequence of measurements performed on an initially prepared single system. Many interesting quantum predictions, such as quantum contextuality or the violation of macroscopic realism, have been demonstrated in this scenario [14–18]. The interplay between information gain and disturbance has been formulated in various tradeoff relation inequalities [19]. The first information theoretic - or entropic - uncertainty relation was formulated by Hirschman [20] in 1957 for the position and momentum observables. This relation was later improved in 1975 by Beckner [21] and Bialynicki-Birula and Mycielski [22]. The extension to non-degenerate observables on a finite-dimensional Hilbert space was then proposed by Deutsch in 1983 [23] and later improved by Maassen and Uffink [24] yielding the well-known entropic uncertainty relation  $H(A) + H(B) \geq -2 \log_2 c$ , where  $H$  denotes the Shannon entropy and  $c$  is the maximal overlap between the eigenvectors  $|a_i\rangle$  and  $|b_j\rangle$  of the observables  $A$  and  $B$ . Entropic uncertainty has useful applications in entanglement witnessing [25], complementarity [26], and in quantum information theory [27]. More general procedures aiming to quantify error and disturbance in successive (or simultaneous) measurements are

Ozawa’s operator-based measures between target observables and measurements [28, 29] or distances of the associated probability distributions [30], proposed by Busch and co-workers. More recently, interest has risen in alternative information-theoretic measures, introduced first by Buscemi [31], but also in several subsequent alternative approaches [32–36].

In the present work, we propose a precise tradeoff relation between correlation and disturbance and present a simple Ramsey-like interferometric implementation in terms of successive neutron spin measurements. Unlike previous approach [31, 37] our scheme captures the mutual incompatibility between the two general measurements in terms of a covariant tradeoff complementarity inequality, meaning the relation is independent of the choice of the coordinate system described by the unitary transformation of the basis. Compared to other approaches [31, 37], our tradeoff relation is based on definitions that are not only functionally simple but also practical for experimental applications. Our work introduces a clear and effective scheme for robust experimental estimation of measurement devices like self-calibration or evaluating the quantum performance of measurement devices. Furthermore, this framework includes a variety of communication protocols such as quantum random access codes and quantum key distribution (QKD), which are applicable in (semi) device-independent quantum communication scenarios, as explored in various other studies [13, 38–44].

*Setup.*— Our setup consists of three parts: a state preparation  $\rho$  followed by two successive observable measurements, denoted by  $\mathcal{M}_a = \sum_{\alpha} \alpha E_{\alpha|a}$  and  $\mathcal{M}_b = \sum_{\beta} \beta E_{\beta|b}$ , respectively. Formally, the general measurements are described by a set of positive operator-valued measures (POVMs) where  $E_{\alpha|a} \geq 0$  and  $\sum_a E_{\alpha|a} = \mathbb{1}$  (see, Fig 1). As is clear from the figure the measurement device  $\mathcal{M}_a$  performs a general measurement operation that not only produces outcomes (classical output) but also realizes the corresponding post-measurement state, according to the transformation rule, described by  $\rho \mapsto \mathcal{I}_{\alpha|a}(\rho) = K_{\alpha|a} \rho K_{\alpha|a}^{\dagger}$  with outcome probability  $p_{\alpha|a} = \text{tr}[\mathcal{I}_{\alpha|a}(\rho)]$  and  $E_{\alpha|a} = K_{\alpha|a}^{\dagger} K_{\alpha|a}$ . Summing over the Kraus operators, i.e.,  $\mathcal{I}_a(\rho) = \sum_{\alpha} \mathcal{I}_{\alpha|a}(\rho)$ ,

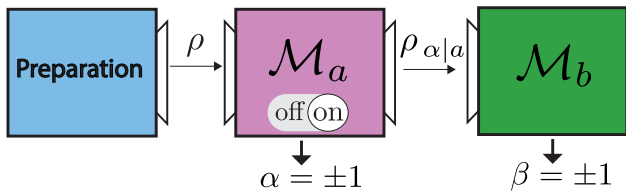


FIG. 1. Ramsey-like interferometric sequence. Schematics of the setup involving three parts: state preparation, successive measurements  $\mathcal{M}_a$  (probe/reference), and measurement  $\mathcal{M}_b$  (target). The measurement disturbance is analyzed via two cases in which measurement  $\mathcal{M}_a$  is turned on (performed) and off (unperformed).

acts as a quantum channel corresponding to the case when the measurement is performed but the outcome is ignored or unregistered. This situation, however, affects the outcome statistics of the subsequent measurement. Therefore, quantum instruments facilitate the analysis of measurement disturbance and incompatibility in sequential measurement setups. The important fact is that the Kraus operators ( $K_{\alpha|a}$ ), generally given by  $K_{\alpha|a} = U_{a|\alpha} E_{\alpha|a}^{\frac{1}{2}}$ , are not unique. We are mainly interested in a particular choice of the instrument associated with the observable measurement effect only and not the unitary afterward, that is  $K_{\alpha|a} = E_{\alpha|a}^{\frac{1}{2}}$  so-called Lüder instrument which merely captures the intrinsic effect of the observable's POVM in the state update rule. Therefore, this special case of instrument is more suitable to study the incompatibility and joint measurability of the observables in sequential implementations [45].

*Correlation-disturbance tradeoff.*— Central to our formulation/construction is the Born rule for evaluating the joint probabilities of the two measurement outcomes:

$$p(\alpha, \beta) = \text{tr} \left[ \mathcal{I}_{\alpha|a}(\rho) E_{\beta|b} \right], \quad (1)$$

which encapsulates the essential information required to analyze the interplay between the two measurements. First, the above form fulfills, the so-called arrow of time, i.e.,  $p(\alpha|a) = \sum_{\beta} p(\alpha, \beta|a, b) = \sum_{\beta} p(\alpha, \beta|a, b')$  for all  $b \neq b'$ , namely, the future measurement will not affect the past measurement.

More characteristically, we have:

$$\tilde{p}(\beta|b) = \text{tr}[\rho \mathcal{I}_a^*(E_{\beta|b})] = \sum_{\alpha} p(\alpha, \beta|a, b), \quad (2)$$

which is equivalent to the scenario where the  $\mathcal{M}_a$  measurement is performed (or turned on) but its outcome is not recorded. Note that this is different from the case in which measurement  $\mathcal{M}_a$  is unperformed (turned off),  $p(b|y) = \text{tr}[\rho E_{b|y}]$ . This means that the difference in the probabilities of obtaining outcome  $\beta$  when it is preceded by the (unregistered)  $\mathcal{M}_a$  measurement, compared to when  $\mathcal{M}_b$  is measured alone, reflects the measurement disturbance [8, 46, 47]. Therefore, a standard distance

measure quantifying the disturbance may given by

$$\mathcal{D} = |\langle \mathcal{M}_b \rangle_{\rho} - \langle \mathcal{I}_a^*(\mathcal{M}_b) \rangle_{\rho}|. \quad (3)$$

Note that the value of  $\mathcal{D}$  depends on the initial state. The maximum value corresponds to the spectral radius norm,  $\mathcal{D} \leq \sup_{\rho} |\mathcal{D}_{\rho}| \leq 1$ , realized for the optimal state maximizing the disturbance detection. The effect of the probe measurement on the target measurement is described by the Lüders channel modifying the observable  $b$  (target), i.e.,  $\mathcal{I}_a^*(\mathcal{M}_b) = \sum_{\alpha} E_{\alpha|a}^{\frac{1}{2}} \mathcal{M}_b E_{\alpha|a}^{\frac{1}{2}}$ . Here  $\mathcal{I}_a^*$  is the dual of a quantum channel preserving the identity operator,  $\mathcal{I}_x^*(\mathbb{1}) = \mathbb{1}$ .

The other measure of interest, defined in terms of (1) is the correlation function:

$$\mathcal{C} = \langle \mathcal{M}_a \mathcal{M}_b \rangle_{\text{seq}} = \sum_{\alpha, \beta} \alpha \beta p(\alpha, \beta|a, b) = \sum_{\alpha} \alpha \langle \mathcal{I}_{\alpha|a}^*(\mathcal{M}_b) \rangle_{\rho} \quad (4)$$

whose absolute value indicates the predictability of the target measurement given the result of the probe(reference) measurement. Although the definitions apply to multiple outcome measurements, as it appears in many cases the most essential features are already captured by two-outcome measurements. Therefore in the present work, we restrict ourselves to dichotomic measurements, i.e.,  $\alpha, \beta = \pm 1$ . In which case the correlation and disturbance, respectively, reduce to  $\mathcal{C} = 2p(\alpha = \beta|a, b) - 1$  and  $\mathcal{D} = 2p(\alpha \neq \beta) - 2\tilde{p}(\alpha \neq \beta)$ .

One naturally expects that the measurement disturbance suppresses the predictability and therefore expect a mutually complementary role between the defined quantities. In the following, we report fundamental statistical constraints between the outcomes of sequential measurements expressed in the form of a tradeoff inequality between correlation and disturbance:

$$\mathcal{C}^2 + \mathcal{D}^2 \leq 1. \quad (5)$$

This inequality, we call  $\mathcal{CD}$ -tradeoff, constituting the starting point of our main result, represents a nontrivial mutual relation: a large correlation implies a small disturbance and vice versa. The mathematical form of (5) appears in a different context known as wave-particle duality relation which has been proposed to illustrate the complementarity between interference visibility and path distinguishability in interferometry, and introduced as a quantum feature independent of Heisenberg uncertainty or noncommutativity [48]. In our sequential measurement setting, however, quantum noncommutativity or incompatibility is indeed taken into account via the measurement disturbance. The sketch of the proof is presented in Supplementary information. To gain a clear geometrical intuition about various specifications and applications of (5), we examine the qubit example and present a precise  $\mathcal{CD}$ -tradeoff holding covariant symmetry proving to be highly useful for the experimental characterization of measurement parameters.

*Qubit case and the covariant symmetry.*— The initial state of a qubit in Bloch representation is  $\rho = \frac{1}{2}(\mathbb{1} + \vec{r} \cdot \vec{\sigma})$  where  $\vec{r}$  is called Bloch vector. The most general form of the two-outcome POVMs for target measurement is  $E_{\pm|b} = ((1 \pm b_0)\mathbb{1} \pm \vec{b} \cdot \vec{\sigma})/2$  giving  $\mathcal{M}_b = E_{+|b} - E_{-|b} = b_0\mathbb{1} + \vec{b} \cdot \vec{\sigma}$  in which  $b_0$  and  $|\vec{b}|$  are interpreted as the measurement *bias* and *sharpness*(strength), respectively, as characteristic parameters describing the measurement apparatus. The positivity condition imposes  $|b_0| + |\vec{b}| \leq 1$ . Given the Bloch representation of the POVM elements and the Lüders channel, the disturbance takes the form  $\mathcal{D} = \langle \vec{b} \cdot \vec{\sigma} \rangle_\rho - \langle \vec{b} \cdot \vec{\sigma} \rangle_\rho = (\vec{b} - \vec{b}') \cdot \vec{r}$  where  $\vec{b}' \cdot \vec{\sigma} = \mathcal{I}_a^*(\vec{b} \cdot \vec{\sigma})$ . As expected, the amount of disturbance depends on the non-commutativity between the corresponding observables,  $\mathcal{D} = -s|\vec{b}| \langle [\hat{a} \cdot \vec{\sigma}, [\hat{a} \cdot \vec{\sigma}, \hat{b} \cdot \vec{\sigma}]] \rangle_\rho = -s|\vec{b}| \hat{a} \times (\hat{a} \times \hat{b}) \cdot \vec{r}$ . Here, the coefficient  $s = 1 - (u_+ + u_-)/2$  where  $u_\alpha = \sqrt{(1 + \alpha a_0)^2 - |\vec{a}|^2}$  accounts for the outcome-dependent *unsharpness* of  $\mathcal{M}_a$  measurement. The above form suggests that the optimal input state maximizing  $\mathcal{D}$  is obtained by a unit Bloch vector  $\vec{r}_{\text{opt}} = (\vec{b} - \vec{b}')/|\vec{b} - \vec{b}'| = -\hat{a} \times (\hat{a} \times \hat{b})$  which lies in the plane spanned by the measurements  $\mathcal{M}_a$  and  $\mathcal{M}_b$  and is perpendicular to the measurement direction of  $\mathcal{M}_a$ , as depicted in Fig. 3 (b), resulting to  $\langle \mathcal{M}_a \rangle = a_0$ . In this case,  $\mathcal{D} = s|\vec{b}| \sin \theta$  where  $\theta = \arccos(\hat{a} \cdot \hat{b})$  represents the angle between the Bloch vectors of the respective measurements. Correlation for the optimal state is expressed as  $\mathcal{C} = a_0 b_0 + |\vec{a}| |\vec{b}| \cos \theta + \delta |\vec{b}| \sin \theta$ . As an example, consider  $\mathcal{M}_x$  being sharp and the second measurement arbitrary then Eq. (6) reduces to an optimal tradeoff,  $\mathcal{C}^2 + \mathcal{D}^2 = |\vec{b}|^2$ . Therefore, one can directly measure the strength of the second measurement by estimating the correlation and disturbance. Note that the form of the relation is invariant under the choice of the measurement settings or the observer's frame of reference, hence called covariant correlation-disturbance.

Consequently, the entire result for the most general pair of measurements can be summarized into the following parametric equations governing the  $\mathcal{CD}$ -tradeoff:

$$\begin{bmatrix} \mathcal{C} \\ \mathcal{D} \end{bmatrix} = \begin{bmatrix} a_0 b_0 \\ 0 \end{bmatrix} + \begin{bmatrix} |\vec{a}| & \delta \\ 0 & s \end{bmatrix} \begin{bmatrix} |\vec{b}| \cos \theta \\ |\vec{b}| \sin \theta \end{bmatrix} \quad (6)$$

where  $\delta = (u_+ - u_-)/2$  is non-zero for bias, introducing shear to the original circle indicating the bias of the reference measurement. The bias of the target measurement is inferred from the displacement  $a_0 b_0$  along the  $x$ -axis. Thus, the values of  $\mathcal{C}$  and  $\mathcal{D}$  follows an ellipse equation encapsulating all essential information about the intrinsic properties of the measurement devices in a generic form, regardless of the unitary transformation of the observables.

By carefully analyzing Eq. (6), we can robustly estimate the characteristics of the measurement devices. In the following, we experimentally demonstrate various instances of the above relationship. The data offers significant validation and verification of the measurement

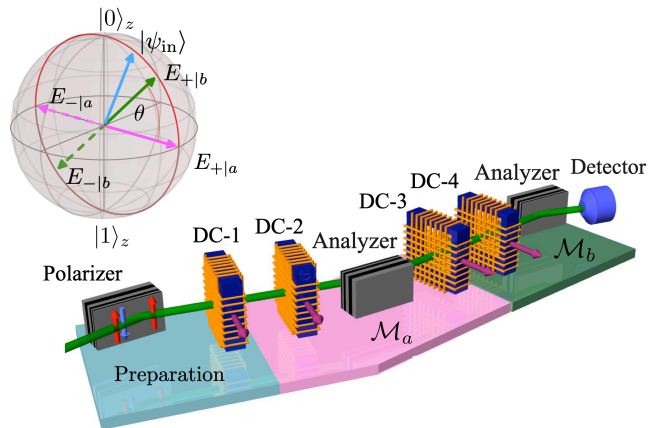


FIG. 2. Neutron optical setup for observation of correlation-disturbance tradeoff relations including Bloch sphere representation of initial state and measured observables. Using supermirrors (polarizer, analyzers) as projection operators and exploiting Larmor recession induced by the magnetic fields and spin turner coils DC-1 to DC-4, any required manipulation of the neutron spin can be performed. Bloch sphere indicates initial state  $|\psi_{\text{in}}\rangle$ , and measurement direction of the first  $\mathcal{M}_a$  and second measurement  $\mathcal{M}_b$ , respectively.

setup's performance by leveraging the covariance symmetry of the  $\mathcal{CD}$ -tradeoff.

*Experimental results.*— The experiment was performed at the 250 kW TRIGA Mark-II research reactor at TU Wien, Austria. A schematic illustration of the experimental setup is depicted in Fig. 2 (see Supplementary Material Sec II A for details). In all our experimental configurations we examine the effects of the first measurement  $\mathcal{M}_a$  on the subsequent measurement  $\mathcal{M}_b$  for the optimal input state  $|\psi_{\text{opt}}\rangle$ , in terms of disturbance  $\mathcal{D}$  and correlations  $\mathcal{C}$ .

First, we implement in our setup the special example in which both measurements are fully projective (labeled as  $\Pi_{\pm|i}$ ). The first measurement is fixed to be  $\mathcal{M}_a = \Pi_{+|a} - \Pi_{-|a} = \sigma_x$ , whereas the second subsequent measurement is set to  $\mathcal{M}_b = \Pi_{+|b}(\theta) - \Pi_{-|b}(\theta) = \cos \theta \sigma_x + \sin \theta \sigma_z$ , with experimentally adjustable parameter  $\theta$ , controlled by the current in DC-4, generating the appropriate magnetic field pointing in  $+y$ -direction. The disturbance is given in theory by  $\mathcal{D} = \sin \theta \langle \sigma_z \rangle_\rho$ . Therefore the optimal input state is  $|\psi_{\text{opt}}\rangle = |0\rangle_z$  for all settings of the controlled parameter  $\theta$ . A complementary form is predicted for the correlation with  $\mathcal{C} = \cos \theta$ . Figure 3 (a) shows a plot of the disturbance  $\mathcal{D}$  versus the correlation  $\mathcal{C}$ ; for  $\theta = 0$ , accounting for a compatible measurement setting of  $\mathcal{M}_a = \sigma_x$  and  $\mathcal{M}_b = \sigma_x$ , we consequently observe zero disturbance  $\mathcal{D}$  and maximal correlation  $\mathcal{C} = 1$ . For the other extreme case  $\theta = \pi/2$  we have maximal disturbance  $\mathcal{D} = 1$  and no more correlations. For all other values  $0 < \theta < \pi/2$  we observe a trade off between  $\mathcal{D}$  and correlation  $\mathcal{C}$ , always fulfilling the tight relation  $\mathcal{C}^2 + \mathcal{D}^2 = 1$ , demonstrating our main results as predicted

in Eq. (6).

Next we investigate the case  $\mathcal{M}_a = \Pi_{+|a}(\theta) - \Pi_{-|a}(\theta) = \vec{b} \cdot \vec{\sigma} = \cos \theta \sigma_x + \sin \theta \sigma_z$  and  $\mathcal{M}_b = \Pi_{+|b} - \Pi_{-|b} = \vec{b} \cdot \vec{\sigma} = \sigma_x$  with associate Bloch vector  $\vec{a} = (\cos \theta, 0, \sin \theta)$  and  $\vec{b} = (1, 0, 0)$ , respectively. Now the optimal initial state  $|\psi_{\text{opt}}\rangle$  is no longer independent of the

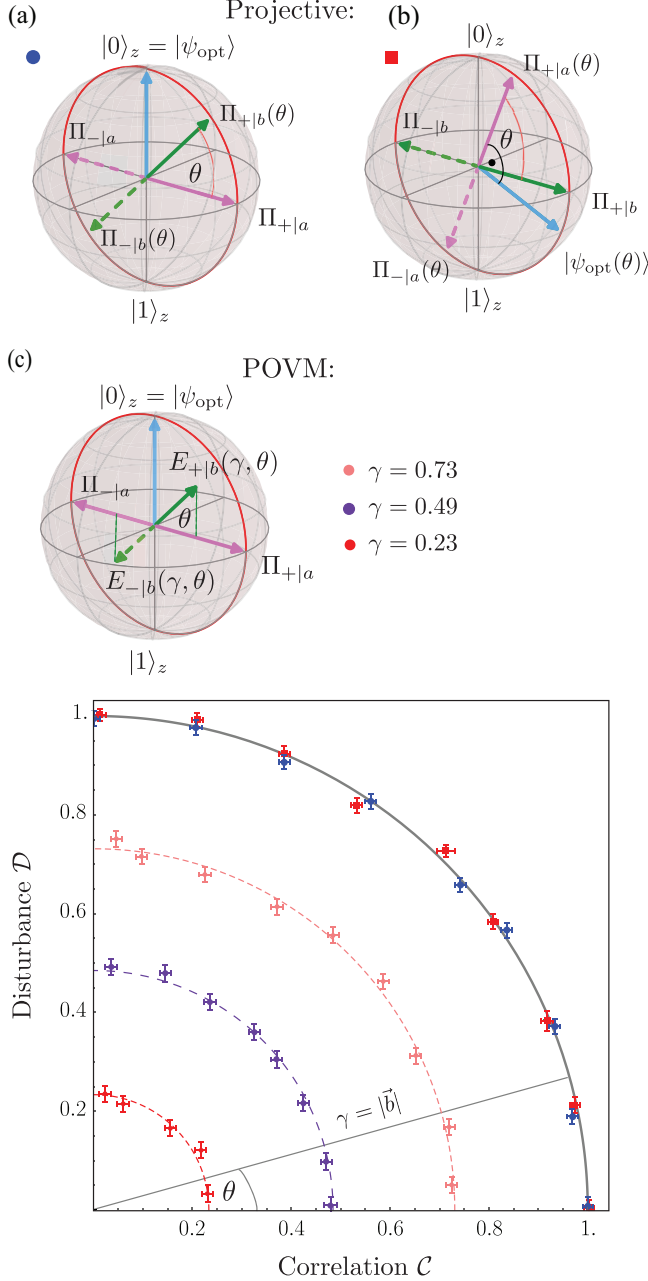


FIG. 3. Disturbance  $\mathcal{D}$  versus correlation  $\mathcal{C}$  with fixed  $\mathcal{M}_a = \sigma_x$  and varying  $\mathcal{M}_b(\theta) = \cos \theta \sigma_x + \sin \theta \sigma_z$  in (a), with fixed  $\mathcal{M}_b = \sigma_x$  and varying  $\mathcal{M}_a(\theta) = \cos \theta \sigma_x + \sin \theta \sigma_z$  and  $|\psi_{\text{opt}}(\theta)\rangle$  in (b). (c) Unsharp measurements with first (fixed) projective  $\mathcal{M}_a = \sigma_x$  and second (rotated) unbiased POVM  $\mathcal{M}_b(\gamma, \theta) = E_{+|b}(\gamma, \theta) - E_{-|b}(\gamma, \theta)$ . The measurement strength  $\gamma$  equals the length of Bloch vector  $\vec{b}$  of the target measurement  $\mathcal{M}_b$ .

control parameter  $\theta$  (see Supplementary Material Sec II D for experimental search of optimal initial state), ensuring their operation within the expected parameters entitled by the covariant symmetry between correlation and disturbance. The plot of disturbance  $\mathcal{D}$  versus the correlation  $\mathcal{C}$  in Fig. 3 (b) shows a similar behaviour as before where the  $\mathcal{M}_a$  measurement was fixed; for  $\theta = 0$  (compatible measurement setting of  $\mathcal{M}_a = \sigma_x$  and  $\mathcal{M}_b = \sigma_x$ ) zero disturbance  $\mathcal{D}$  and maximal correlation  $\mathcal{C} = 1$  are observed. For the other extreme case  $\theta = \pi/2$  we have maximal disturbance  $\mathcal{D} = 1$  and no more correlations. For all other values  $0 < \theta < \pi/2$  the covariance between  $\mathcal{D} = \cos \theta$  and correlation  $\mathcal{C} = \sin \theta$  fulfills the tight relation  $\mathcal{C}^2 + \mathcal{D}^2 = 1$ , as a special case of Eq. (6) demonstrating our main result.

For a better understanding of the implementation of a general measurement process in our setup, it is useful to rewrite the POVM in the following form

$$E_{\pm|b}(\theta, \gamma, b_0) = \gamma \Pi_{\pm}(\theta) + (1 - \gamma) N_{\pm}(b_0) \quad (7)$$

as a convex combination of projective measurement  $\Pi_{\pm}(\theta) = (\mathbb{1} \pm \hat{b}(\theta) \cdot \vec{\sigma})/2$ , with unit vector  $\hat{b}(\theta)$ , and biased dummy (noisy) measurement  $N_{\pm}(b_0) = \frac{1}{2}(\mathbb{1} \pm \frac{b_0}{1-\gamma})\mathbb{1}$ , which is fully characterized by three parameters, rotation angle  $\theta$  about a specific axes, bias  $b_0$ , and the randomization degree  $\gamma$ . In the qubit case  $\gamma = |\vec{b}|$ . If  $b_0 = 0$  the POVM is unbiased (see Supplemental Material Sec II B for the experimental implementation of POVMs). First we study the case where the probe (first) measurement is projective and given by  $\mathcal{M}_a = \sigma_x$ , while the target (second) measurement is represented by the unbiased POVM  $\mathcal{M}_b(\gamma, \theta) = E_{+|b}(\gamma, \theta) - E_{-|b}(\gamma, \theta)$ , with POVM elements  $\Pi_{\pm|b}(\gamma, \theta)$  from Eq. (S.4). The resulting tight trade off relation (Eq. (6))  $\mathcal{C}^2 + \mathcal{D}^2 = |\vec{b}|^2$  can be seen in Fig. 3 (d). This particular configurations allows for a direct determination of the measurement strength  $\gamma$  and in turn for the Bloch length  $|\vec{b}|$ . This self-calibration or *self-testing* feature results in the following experimentally determined interaction strengths  $\gamma$ :  $\gamma_1 = 0.731(4)$ ,  $\gamma_2 = 0.485(3)$ , and  $\gamma_3 = 0.233(3)$ , which is plotted in Fig. 3 (d) in red, violet and magenta, respectively. In a configuration where the POVM is the last measurement the bias  $b_0$  has no effect. The practical advantage of this finding becomes more significant for higher dimensional measurement in which the readout noise or detector precision is estimated without resorting to highly demanding process tomography (see Supplementary Material Sec II C for details of higher dimensional measurement).

Thus, next we reverse the order of POVM and projective measurement; now the probe (first) measurement is the POVM  $\mathcal{M}_a(\gamma) = E_{+|a}(\gamma) - E_{-|a}(\gamma)$  and the target (second) measurement is projective given by  $\mathcal{M}_b(\theta) = \cos \theta \sigma_x + \sin \theta \sigma_z$ . As seen from Fig. 4 the (unbiased) unsharp measurement disturbs the second measurement less compared to a projective measurement, which results in an elliptic shape, as defined in Eq. (6), of the correlation-disturbance tradeoff, which is plotted in

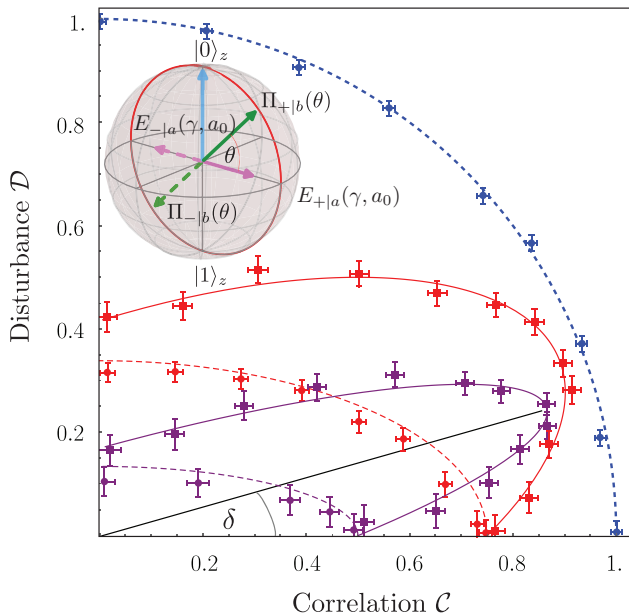


FIG. 4. Disturbance  $\mathcal{D}$  versus correlation  $\mathcal{C}$  with first unbiased and biased POVM  $\mathcal{M}_a(\gamma, a_0) = E_{+|a}(\gamma, a_0) - E_{-|a}(\gamma, a_0)$  and second (varying) projective  $\mathcal{M}_b(\theta) = \cos \theta \sigma_x + \sin \theta \sigma_z$ .

red and purple for interaction strengths  $\gamma = 0.5$  and  $\gamma = 0.75$ , respectively. Finally, the effect of a biased POVM is studied, where according to Eq. (6) in addition the elliptic shape of the correlation-disturbance relation a tilt  $\delta$  occurs, which is plotted in Fig. 4 for  $\gamma = 0.5, a_0 = 0.5$  and  $\gamma = 0.75, a_0 = 0.25$  as red and purple squares, respectively.

At this point we want to emphasize that since the discussed tradeoff relation is invariant under the unitary transformation of the observables, which means that measurement settings (e.g. measurement direction  $\theta$ ) do not have to be known in principle, our result offers an experimentally robust estimation or character-

ization of the certain measurement parameters such as the measurement strength  $\gamma$  even with limited control over the measurements, and in situations involving uncharacterized local unitary noise. This paves the way for self-calibration of quantum measurement devices in (semi) device-independent quantum communication applications.

*Conclusion and outlook.*— The correlation  $\mathcal{C}$  and the disturbance  $\mathcal{D}$  induced by quantum measurements are not independent quantities; they are mutually related in a nontrivial way. The precise form of this relationship, presented in this work, reflects the covariant symmetric interplay between the two quantities. Exploiting these symmetries provides a robust tool for estimating characteristic parameters of measurement devices, such as sharpness and bias with clear practical application in High-dimensional setting. Our experimental implementation demonstrates the theoretical derivations with high precision, showing that the interplay between  $\mathcal{C}$  and  $\mathcal{D}$  closely adheres to the predicted relation.

Furthermore, to motivate our study towards a more fundamental analysis, we anticipate that optimal choices of disturbance, as a means of transmitting information, and correlation, as a measure of predictability, could outperform or even rule out certain classical (hidden variable) models. Leveraging this argument, our protocol offers a new perspective on the extent of nonclassical behavior implied by quantum uncertainties [49]. This approach aligns with schemes of two-time Leggett-Garg macroscopic realism [50], sequential random access codes and self-testing of measurement instruments [38–40, 51, 52]. Consequently, our straightforward Ramsey interferometric scheme could be effectively adapted to optical-based quantum information tasks where quantum (communication) advantage over classical counterparts is highlighted.

*Acknowledgments.*— We are grateful to M. Huber and G. Vitagliano for the interesting discussion and useful comments. This work was supported by the Austrian science fund (FWF) Project No. P 34239.

- 
- [1] W. Heisenberg, Über den anschaulichen Inhalt der quantentheoretischen Kinematik und Mechanik, *Z. Phys.* **43**, 172 (1927).
- [2] P. Busch, P. Lahti, and R. F. Werner, Colloquium: Quantum root-mean-square error and measurement uncertainty relations, *Rev. Mod. Phys.* **86**, 1261 (2014).
- [3] N. BOHR, The quantum postulate and the recent development of atomic theory, *Nature* **121**, 580 (1928).
- [4] J. S. Bell, On the Einstein-Podolsky-Rosen paradox, *Physics (Long Island City, N.Y.)* **1**, 195 (1964).
- [5] J. S. Bell, On the problem of hidden variables in quantum mechanics, *Rev. Mod. Phys.* **38**, 447 (1966).
- [6] S. Kochen and E. P. Specker, The problem of hidden variables in quantum mechanics, *J. Math. Mech.* **17**, 59 (1967).
- [7] M. M. Wolf, D. Perez-Garcia, and C. Fernandez, Measurements incompatible in quantum theory cannot be measured jointly in any other no-signaling theory, *Phys. Rev. Lett.* **103**, 230402 (2009).
- [8] O. Gühne, E. Haapasalo, T. Kraft, J.-P. Pellonpää, and R. Uola, Colloquium: Incompatible measurements in quantum information science, *Rev. Mod. Phys.* **95**, 011003 (2023).
- [9] F. Arute *et. al.*, Quantum supremacy using a programmable superconducting processor, *Nature* **574**, 505 (2019).
- [10] K. Sen, S. Halder, and U. Sen, Incompatibility of local quantum measurements providing an advantage in local quantum state discrimination, *Phys. Rev. A* **109**, 012415 (2024).
- [11] D. F. V. James, P. G. Kwiat, W. J. Munro, and A. G. White, Measurement of qubits, *Phys. Rev. A* **64**, 052312 (2001).
- [12] F. B. Maciejewski, Z. Zimborás, and M. Oszmaniec, Mitigation of readout noise in near-term quantum devices by

- classical post-processing based on detector tomography, *Quantum* **4**, 257 (2020).
- [13] A. Elben, S. T. Flammia, H.-Y. Huang, R. Kueng, J. Preskill, B. Vermersch, and P. Zoller, The randomized measurement toolbox, *Nature Reviews Physics* **5**, 9 (2023).
- [14] A. J. Leggett and A. Garg, Quantum mechanics versus macroscopic realism: Is the flux there when nobody looks?, *Phys. Rev. Lett.* **54**, 857 (1985).
- [15] C. Emary, N. Lambert, and F. Nori, Leggett–Garg inequalities, *Reports on Progress in Physics* **77**, 016001 (2013).
- [16] G. C. Knee, K. Kakuyanagi, M.-C. Yeh, Y. Matsuzaki, H. Toida, H. Yamaguchi, S. Saito, A. J. Leggett, and W. J. Munro, A strict experimental test of macroscopic realism in a superconducting flux qubit, *Nature Communications* **7**, 13253 (2016).
- [17] E. Kreuzgruber, R. Wagner, N. Geerits, H. Lemmel, and S. Sponar, Violation of a Leggett–Garg inequality using ideal negative measurements in neutron interferometry, *Phys. Rev. Lett.* **132**, 260201 (2024).
- [18] G. Vitagliano and C. Budroni, Leggett–Garg macrorealism and temporal correlations, *Phys. Rev. A* **107**, 040101 (2023).
- [19] C. A. Fuchs and A. Peres, Quantum-state disturbance versus information gain: Uncertainty relations for quantum information, *Phys. Rev. A* **53**, 2038 (1996).
- [20] I. I. Hirschman, A note on entropy, *Am. J. Math.* **79**, 152 (1957).
- [21] W. Beckner, Inequalities in fourier analysis, *Annals of Mathematics* **102**, 159 (1975).
- [22] I. Białynicki-Birula and J. Mycielski, Uncertainty relations for information entropy in wave mechanics, *Commun. Math. Phys.* **44**, 129 (1975).
- [23] D. Deutsch, Uncertainty in quantum measurements, *Phys. Rev. Lett.* **50**, 631 (1983).
- [24] H. Maassen and J. B. M. Uffink, Generalized entropic uncertainty relations, *Phys. Rev. Lett.* **60**, 1103 (1988).
- [25] M. Berta, M. Christandl, R. Colbeck, J. M. Renes, and R. Renner, The uncertainty principle in the presence of quantum memory, *Nature Physics* **6**, 659 (2010).
- [26] P. J. Coles, J. Kaniewski, and S. Wehner, Equivalence of wave-particle duality to entropic uncertainty, *Nature Communications* **5**, 5814 (2014).
- [27] M. A. Nielsen and I. Chuang, *Quantum Computation and Quantum Information*, edited by M. A. Nielsen and I. Chuang, Cambridge University Press, Cambridge (2000).
- [28] M. Ozawa, Universally valid reformulation of the Heisenberg uncertainty principle on noise and disturbance in measurement, *Phys. Rev. A* **67**, 042105 (2003).
- [29] M. Ozawa, Uncertainty relations for noise and disturbance in generalized quantum measurements, *Ann. Phys.* **311**, 350.
- [30] R. F. Werner, The uncertainty relation for joint measurement of position and momentum, *Quant. Inf. Comput.* **4**, 546 (2004).
- [31] F. Buscemi, M. J. Hall, M. Ozawa, and M. M. Wilde, Noise and disturbance in quantum measurements: An information-theoretic approach, *Phys. Rev. Lett.* **112**, 050401 (2014).
- [32] P. J. Coles and F. Furrer, State-dependent approach to entropic measurement–disturbance relations, *Physics Letters A* **379**, 105 (2015).
- [33] K. Baek and W. Son, Entropic uncertainty relations for successive generalized measurements, *Mathematics* **4**, 10.3390/math4020041 (2016).
- [34] R. Schwonnek, D. Reeb, and R. F. Werner, Measurement uncertainty for finite quantum observables, *Mathematics* **4**, 10.3390/math4020038 (2016).
- [35] A. Barchielli, M. Gregoratti, and A. Toigo, Measurement uncertainty relations for discrete observables: Relative entropy formulation, *Communications in Mathematical Physics* **357**, 1253 (2018).
- [36] N. Saberian, S. J. Akhtarshenas, and F. Shahbeigi, Measurement sharpness and disturbance tradeoff, *Phys. Rev. A* **109**, 012201 (2024).
- [37] P. Busch, P. Lahti, and R. F. Werner, Colloquium: Quantum root-mean-square error and measurement uncertainty relations, *Rev. Mod. Phys.* **86**, 1261 (2014).
- [38] K. Mohan, A. Tavakoli, and N. Brunner, Sequential random access codes and self-testing of quantum measurement instruments, *New Journal of Physics* **21**, 083034 (2019).
- [39] N. Miklin, J. J. Borkala, and M. Pawłowski, Semi-device-independent self-testing of unsharp measurements, *Phys. Rev. Res.* **2**, 033014 (2020).
- [40] H. Anwer, S. Muhammad, W. Cherifi, N. Miklin, A. Tavakoli, and M. Bourennane, Experimental characterization of unsharp qubit observables and sequential measurement incompatibility via quantum random access codes, *Phys. Rev. Lett.* **125**, 080403 (2020).
- [41] P. Roy and A. K. Pan, Device-independent self-testing of unsharp measurements, *New Journal of Physics* **25**, 013040 (2023).
- [42] R. Stricker, D. Vodola, A. Erhard, L. Postler, M. Meth, M. Ringbauer, P. Schindler, R. Blatt, M. Müller, and T. Monz, Characterizing quantum instruments: From nondemolition measurements to quantum error correction, *PRX Quantum* **3**, 030318 (2022).
- [43] S.-L. Chen and J. Eisert, Semi-device-independently characterizing quantum temporal correlations, *Phys. Rev. Lett.* **132**, 220201 (2024).
- [44] S. Gherardini and G. De Chiara, Quasiprobabilities in quantum thermodynamics and many-body systems, *PRX Quantum* **5**, 030201 (2024).
- [45] T. Heinosaari and T. Miyadera, Universality of sequential quantum measurements, *Phys. Rev. A* **91**, 022110 (2015).
- [46] R. Uola, G. Vitagliano, and C. Budroni, Leggett–garg macrorealism and the quantum nondisturbance conditions, *Phys. Rev. A* **100**, 042117 (2019).
- [47] G. Schild and C. Emary, Maximum violations of the quantum-witness equality, *Phys. Rev. A* **92**, 032101 (2015).
- [48] B.-G. Englert, Fringe visibility and which-way information: An inequality, *Phys. Rev. Lett.* **77**, 2154 (1996).
- [49] L. Catani, M. Leifer, G. Scala, D. Schmid, and R. W. Spekkens, What is nonclassical about uncertainty relations?, *Phys. Rev. Lett.* **129**, 240401 (2022).
- [50] J. J. Halliwell, Leggett–garg inequalities and no-signaling in time: A quasiprobability approach, *Phys. Rev. A* **93**, 022123 (2016).
- [51] S. Wagner, J.-D. Bancal, N. Sangouard, and P. Sekatski, Device-independent characterization of quantum instruments, *Quantum* **4**, 243 (2020).
- [52] S.-L. Chen and J. Eisert, Semi-device-independently characterizing quantum temporal correlations, *Phys. Rev. Lett.* **132**, 220201 (2024).

## Appendix A: Supplementary Material

This Supplemental Material provides the theoretical derivation of the main result and also the experimental detail on determination of the optimal initial state and properties of the post-measurement state.

## Appendix B: Theoretical Details

### 1. General qubit measurement

The spectral decomposition of the Positive Operator-Valued Measure (POVM) elements for a general dichotomic measurement is given by

$$E_+ = \sum_{j=1}^2 p_j |j\rangle\langle j|, \quad E_- = \mathbb{1} - E_+ = \sum_{j=1}^2 q_j |j\rangle\langle j|, \quad (\text{S.1})$$

where  $q_j = 1 - p_j$ . This describes how  $E_+$  and  $E_-$  are built from projectors  $|j\rangle\langle j|$  with probabilities  $p_j$  and  $q_j$ , ensuring  $E_+ + E_- = \mathbb{1}$ . This leads to the relation:

$$E_{\pm|b} = \frac{\mathbb{1} \pm \mathcal{M}_b}{2}, \quad \mathcal{M}_b = b_0 \mathbb{1} + |\vec{b}\rangle\langle \vec{b}|, \quad (\text{S.2})$$

where  $\mathcal{M}_b$  is parameterized by the four-vector  $(b_0, \vec{b})$ , and similarly for  $\mathcal{M}_a$  with  $(a_0, \vec{a})$ .

A useful form for general two-outcome POVMs, such as  $\mathcal{M}_a$  and  $\mathcal{M}_b$ , is:

$$E_{\pm|b} = |\vec{b}\rangle\langle \vec{b}| \Pi_{\pm|b} + (1 - |\vec{b}\rangle\langle \vec{b}|) N_{\pm|b}, \quad (\text{S.3})$$

where  $E_{\pm|b}$  is decomposed into a projection term  $\Pi_{\pm|b}$  and a noise term  $N_{\pm|b}$ , known as randomizing the measurement.

Finally, the joint probability for two outcomes  $(+, +)$  is:

$$p(+, +) = \text{tr} [\mathcal{I}_{\alpha|a}(\rho) E_{\beta|b}], \quad (\text{S.4})$$

where  $\mathcal{I}_{\alpha|a}(\rho)$  is the post-measurement state conditioned on outcome  $\alpha$  for measurement  $a$ , and  $E_{\beta|b}$  is the POVM element for outcome  $\beta$  of measurement  $b$ .

### 2. An explicit derivations & Proof of the inequality

First, let's define the disturbance operator  $\hat{d}$  and the disturbance  $\mathcal{D}$  as:

$$\hat{d} = \mathcal{M}_b - \mathcal{I}_a^*(\mathcal{M}_b), \quad \mathcal{D} = \langle \hat{d} \rangle_\rho, \quad (\text{S.5})$$

where  $\mathcal{I}_a^*(\mathcal{M}_b)$  is the action of the Lüders channel on  $\mathcal{M}_b$ , given by:

$$\mathcal{I}_a^*(\mathcal{M}_b) = \sum_{\alpha} \mathcal{I}_\alpha^*(\mathcal{M}_b) = \sum_{\alpha} E_\alpha^{\frac{1}{2}} \mathcal{M}_b E_\alpha^{\frac{1}{2}}. \quad (\text{S.6})$$

A useful trick is to decompose the Lüders channel into two terms:

$$\mathcal{I}_\alpha^*(\mathcal{M}_b) = \frac{1}{2} \{E_\alpha, \mathcal{M}_b\} - \mathcal{L}_\alpha^*(\mathcal{M}_b), \quad (\text{S.7})$$

where the second term,  $\mathcal{L}_\alpha^*(\mathcal{M}_b)$ , often referred to as the dissipator, accounts for the disturbance:

$$\mathcal{L}_\alpha^*(\mathcal{M}_b) = \frac{1}{2} [E_\alpha^{\frac{1}{2}}, [E_\alpha^{\frac{1}{2}}, \mathcal{M}_b]] = [E_\alpha^{\frac{1}{2}}, [E_\alpha^{\frac{1}{2}}, E_{+|b}]]. \quad (\text{S.8})$$

Thus, we can express the disturbance operator  $\hat{d}$  as:

$$\hat{d} = \mathcal{L}_{+|a}^*(\mathcal{M}_b) + \mathcal{L}_{-|a}^*(\mathcal{M}_b) = 2 [E_a^{\frac{1}{2}}, [E_a^{\frac{1}{2}}, E_{+|b}]], \quad (\text{S.9})$$

Note that the above derivations are general and apply to arbitrary dichotomic measurements in  $d$ -dimensional Hilbert space.

Now, more explicitly, for a general two-outcome qubit POVM:

$$\hat{d} = |\vec{b}\rangle\langle \vec{b}| \left( \mathcal{L}_{+|a}^*(\hat{b} \cdot \vec{\sigma}) + \mathcal{L}_{-|a}^*(\hat{b} \cdot \vec{\sigma}) \right). \quad (\text{S.10})$$

The following relation simplifies the derivation:

$$(\vec{a} \cdot \vec{\sigma})(\vec{b} \cdot \vec{\sigma}) = \vec{a} \cdot \vec{b} \mathbb{1} + i(\vec{a} \times \vec{b}) \cdot \vec{\sigma}. \quad (\text{S.11})$$

Using this, the dissipator  $\mathcal{L}_\alpha^*(\mathcal{M}_b)$  can be simplified as:

$$\mathcal{L}_\alpha^*(\mathcal{M}_b) = \frac{a_\alpha s_\alpha |\vec{b}|}{2} (\hat{a} \times (\hat{a} \times \hat{b})) \cdot \sigma, \quad (\text{S.12})$$

where  $a_\pm = 1 \pm a_0$  and  $s_\pm = 1 - \sqrt{1 - \frac{|\vec{a}|^2}{a_\pm^2}}$ . The term  $s$  is then:

$$s = \frac{1}{2}(a_+ s_+ + a_- s_-) = 1 - \frac{1}{2}(u_+ + u_-), \quad (\text{S.13})$$

where, as defined earlier,  $u_\alpha = \sqrt{a_\alpha^2 - |\vec{a}|^2}$ . For unbiased POVMs, we have  $a_\pm = 1 - \sqrt{1 - |\vec{a}|^2}$ . Therefore, the disturbance  $\mathcal{D}$  for the optimal state is:

$$\mathcal{D} = s |\vec{b}| \sin \theta. \quad (\text{S.14})$$

We also need to simplify the following expression:

$$\frac{1}{2}(a_+ s_+ - a_- s_-) = a_0 + \delta, \quad (\text{S.15})$$

where  $\delta = \frac{1}{2}(u_+ - u_-)$  represents the measurement bias.

The correlation, denoted by  $\mathcal{C} = \text{tr}(\rho \hat{C})$ , can be written as:

$$\hat{C} = \sum_{\alpha} \alpha \mathcal{I}_\alpha^*(\mathcal{M}_b), \quad (\text{S.16})$$

which can be expanded as:

$$\hat{C} = \frac{1}{2} \{ \mathcal{M}_a, \mathcal{M}_b \} - \left( \mathcal{L}_{+|a}^*(\mathcal{M}_b) - \mathcal{L}_{-|a}^*(\mathcal{M}_b) \right), \quad (\text{S.17})$$

or, more explicitly for qubit POVM:

$$\hat{C} = \frac{1}{2}\{\mathcal{M}_a, \mathcal{M}_b\} - |\vec{b}\rangle\left(\mathcal{L}_{+|a}^*(\hat{b} \cdot \vec{\sigma}) - \mathcal{L}_{-|a}^*(\hat{b} \cdot \vec{\sigma})\right). \quad (\text{S.18})$$

Using these relations, the correlation for the optimal prepared state becomes:

$$\mathcal{C} = a_0 b_0 + |\vec{a}||\vec{b}| \cos \theta + \delta |\vec{b}| \sin \theta. \quad (\text{S.19})$$

The trade-off between correlation  $\mathcal{C}$  and disturbance  $\mathcal{D}$  is given by the following parametric equations:

$$\begin{bmatrix} \mathcal{C} \\ \mathcal{D} \end{bmatrix} = \begin{bmatrix} a_0 b_0 \\ 0 \end{bmatrix} + \begin{bmatrix} |\vec{a}| & \delta \\ 0 & s \end{bmatrix} \begin{bmatrix} |\vec{b}| \cos \theta \\ |\vec{b}| \sin \theta \end{bmatrix}. \quad (\text{S.20})$$

This formulation captures the unsharpness and bias of the probe measurement  $\mathcal{M}_a$  through a combined transformation that performs both skewing (shearing) and scaling (squeezing) on the original circle. Here,  $\delta$  is the shear factor, quantifying the measurement bias.

We can proceed with further simplifications. The expression:

$$|\vec{a}||\vec{b}| \cos \theta + \delta |\vec{b}| \sin \theta \quad (\text{S.21})$$

can be simplified into a single cosine term:

$$R \cos(\theta - \phi), \quad (\text{S.22})$$

where

$$R = |\vec{b}| \sqrt{|\vec{a}|^2 + \delta^2} \quad (\text{the amplitude}), \quad (\text{S.23})$$

$$\tan \phi = \frac{\delta}{|\vec{a}|} \quad (\text{the phase shift}). \quad (\text{S.24})$$

This derivation resembles elliptical polarization.

Correlation and disturbance can generally be expressed as

$$\mathcal{C} = \lambda u_0 + (1 - \lambda)v, \quad \mathcal{D} = \lambda u_1, \quad (\text{S.25})$$

where the square of  $\mathcal{C}$  and  $\mathcal{D}$  are given by:

$$\mathcal{C}^2 = \lambda^2 u_0^2 + 2\lambda(1 - \lambda)u_0 v + (1 - \lambda)^2 v^2, \quad (\text{S.26})$$

$$\mathcal{D}^2 = \lambda^2 u_1^2. \quad (\text{S.27})$$

Then,

$$\mathcal{C}^2 + \mathcal{D}^2 \leq \lambda^2 \|u\|^2 + 2\lambda(1 - \lambda)u_0 v + (1 - \lambda)^2 v^2 \quad (\text{S.28})$$

$$\leq \left(\lambda \|u\| + (1 - \lambda)v\right)^2 \leq 1, \quad (\text{S.29})$$

where we use  $\|u\|^2 = u_0^2 + u_1^2$ .

The inequality holds because  $u_0 \leq \sqrt{1 - u_1^2}$ , implying  $u_0 \leq \|u\| \leq 1$ .

### 3. Generalization to two-outcome measurements in $d$ -dimensional Hilbert space

The spectral decomposition of the POVM elements for a general dichotomic measurement in a  $d$ -dimensional Hilbert space is given by

$$E_+ = \sum_{j=1}^d p_j |j\rangle\langle j|, \quad E_- = \mathbb{1} - E_+ = \sum_{j=1}^d q_j |j\rangle\langle j|, \quad (\text{S.30})$$

where  $q_j = 1 - p_j$ .

A specific example is a randomized measurement that decomposes as a projection plus a noise term proportional to the identity:

$$E_+ = \gamma \Pi_+ + (1 - \gamma)N_+, \quad E_- = \mathbb{1} - E_+, \quad (\text{S.31})$$

where  $\gamma$  quantifies the measurement's sharpness or precision.

In the case where the first measurement is sharp and the second measurement follows the above form, the disturbance operator  $\hat{d}$  is given by

$$\hat{d} = \gamma \sum_{\alpha} \left( \{\Pi_{\alpha}, \Pi_{+|b}\} - 2\Pi_{\alpha}\Pi_{+|b}\Pi_{\alpha} \right) \quad (\text{S.32})$$

$$= 2\gamma \left( \{\Pi_{+|a}, \Pi_{+|b}\} - 2\Pi_{+|a}\Pi_{+|b}\Pi_{+|a} \right). \quad (\text{S.33})$$

Operator  $\{\Pi_{+|a}, \Pi_{+|b}\} - 2\Pi_{+|a}\Pi_{+|b}\Pi_{+|a}$  is a traceless rank-two matrix, meaning that its eigenvalues are  $\pm\lambda$  and 0. Thus, we can express the spectral decomposition of  $\hat{d}$  as

$$\hat{d} = \gamma \left[ \lambda |\psi_+\rangle\langle\psi_+| - \lambda |\psi_-\rangle\langle\psi_-| \right], \quad (\text{S.34})$$

where

$$\lambda = 2\sqrt{(1 - c^2)c^2}, \quad c^2 = \text{tr}(\Pi_{+|a}\Pi_{+|b}). \quad (\text{S.35})$$

The maximum value of disturbance,  $\lambda = 1$ , is reached when  $c^2 = \frac{1}{2}$ . Note that,

$$\Pi_{+|a} = |v_a\rangle\langle v_a|, \quad \Pi_{+|b} = |v_b\rangle\langle v_b| \quad (\text{S.36})$$

and  $|\langle\psi_+|v_a\rangle| = \frac{1}{\sqrt{2}}$  and consequently, we obtain

$$\langle\mathcal{M}_a\rangle = 0. \quad (\text{S.37})$$

Note that the optimal state is such that the value of the disturbance solely depends on the overlap between the projectors of the corresponding measurements.

$$\mathcal{D} = \langle\psi_+|\hat{d}|\psi_+\rangle = 2\gamma\sqrt{(1 - c^2)c^2} \quad (\text{S.38})$$

and for the correlation

$$\mathcal{C} = \langle\psi_+|\hat{C}|\psi_+\rangle = \gamma(2c^2 - 1). \quad (\text{S.39})$$

This yields the relation

$$\mathcal{C}^2 + \mathcal{D}^2 = \gamma^2, \quad (\text{S.40})$$

satisfying a circle in the  $\mathcal{C}$ - $\mathcal{D}$  plane. Further, we can directly estimate the Bloch length of the second measurement as  $|\vec{b}| = \gamma\sqrt{d-1}$ . This length is chosen such that for a basis operator, the orthogonality condition  $\text{tr}(\sigma_i\sigma_j) = d\delta_{ij}$  holds and thus  $0 \leq |\vec{b}| \leq \sqrt{d-1}$ .



## Appendix C: Experimental Details

### 1. Experimental Setup

The experiment was carried out at the polarimeter instrument *NepTUn* (*NEutron Polarimeter TU wieN*), located at the tangential beam port of the 250 kW TRIGA Mark II research reactor at the Atominstitut - TU Wien, in Vienna, Austria. As in several previous experiments the qubit system studied in the present experiment is represented by the spin, a *two-state system*, of the spin-1/2 particle neutron, where  $\mathcal{S}_i = \frac{\hbar}{2} \sigma_i$ , with  $i = x, y, z$ . An unpolarized thermal neutron beam is monochromatized via Bragg-reflection from a pyrolytic graphite crystal, having a mean wavelength of 2.02 Å and spectral width  $\Delta\lambda/\lambda = 0.015$ . Next, the beam is spin-polarized up to  $\sim 99\%$  in  $+z$ -direction by reflection from a bent Co-Ti supermirror array thus yielding spin state  $|+z\rangle$ . In order to manipulate the neutron's spin state magnetic fields are applied which interact with the neutron via the Zeeman Hamiltonian  $\mu\vec{\sigma}\vec{B}$ . The action of a static magnetic field pointing in direction  $\vec{n}_B$  on the neutron's spin state is described by the unitary transformation  $U_R = e^{i\alpha\vec{n}_B\vec{\sigma}}$ , with  $\alpha = \mu|B|T/\hbar$  and  $\vec{\sigma} = (\sigma_x, \sigma_y, \sigma_z)^T$ , where  $\sigma_{x,y,z}$  are the Pauli spin operators. Here,  $\mu$  denotes the magnetic moment of the neutron,  $|B|$  is the modulus of the magnetic field strength, and  $T$  is the time of flight through the field region. Thus, the static magnetic field induces a rotation of the neutron's polarization vector, i.e., the neutron's Bloch vector, around the axis  $\vec{n}_B$  of the magnetic field, with frequency  $\omega_L = |2\mu B/\hbar|$ , which is referred to as Larmor precession. For thermal neutrons, the effects of the magnetic field on the spatial part of the neutron's wave function (longitudinal Stern - Gerlach effect) are negligible. To prevent depolarization by stray fields, a guide field  $B_z^{\text{GF}}$  pointing in the positive  $z$ -direction having a magnitude of 13 Gauss, from coils in Helmholtz configuration, is applied along the entire setup.

For the preparation of arbitrary input states  $|\psi_{\text{in}}\rangle$  a so-called spin rotator coil DC-1 is used which produces a static magnetic field  $B_y$  pointing in  $+y$ -direction. The Bloch vector of the incident neutrons thus experiences Larmor precession around the  $y$ -axis while passing through the coil. By setting the coil's field strength the Bloch vector's polar angle is set to the required value.

For the projective measurement of a spin observable  $\mathcal{M}_a = 2M_{+|a} - \mathbb{1}$  its projection operators  $M_{+,\pm|a}$  have to be realized in the actual experiment. We illustrate this procedure for the case  $\mathcal{M}_a = \sigma_x$  (and as well for  $\mathcal{M}_a = \cos\theta\sigma_x + \sin\theta\sigma_z$ ) in Fig. 2 of the main text. Therefore, a second spin turner coil, denoted as DC-2, with a magnetic field pointing in  $+y$ -direction is utilized. The field strength of DC-2 is chosen such that exactly the  $|+x\rangle$  ( $|+\theta\rangle$ ) component of the initially prepared state is rotated onto  $|+z\rangle$ . Next, another supermirror array (first analyzer) only allows neutrons in  $|+z\rangle$  spin state to pass thus acting as projector  $|+z\rangle\langle+z|$ . From the  $|+z\rangle$  state exiting the supermirror  $|+z\rangle$  is gener-

ated by using another spin turner coil (DC-3). Analogously to the initial state preparation with DC-1, DC-3's field strength adjusts the polar angle of the neutron's Bloch vector to complete the projective measurement, with *post-measurement state* being an eigenstate of  $\mathcal{M}_a$  (unsharp measurements are discussed in the next Section).

The subsequent measurement of  $\mathcal{M}_b = 2M_{+|b} - \mathbb{1}$  is performed similarly with spin turner coil DC-4 and a second supermirror analyzer. A final preparation of the eigenstates of  $\mathcal{M}_b = 2M_{+|b} - \mathbb{1}$  is not required since the  $\text{BF}_3$  counting detector is insensitive to spin states. To compensate for random fluctuations of the reactor's neutron flux an additional  $^3\text{He}$  monitor detector, mounted in front of the actual setup, is used to normalize the count rate.

### 2. POVM implementation

As described in the main text general measurements are expressed by

$$E_{\pm|b}(\theta, \gamma, b_0) = (1 - \gamma)N_{\pm}(b_0) + \gamma\Pi_{\pm}(\theta) \quad (\text{S.1})$$

as a convex combination of projective  $\Pi_{\pm}(\theta)$  and biased dummy measurement  $N_{\pm}(b_0) = \frac{1}{2}(1 \pm \frac{b_0}{1-\gamma})\mathbb{1}$ , which is fully characterized by three parameters,  $\theta$ ,  $\gamma$ , and  $b_0$ , see Fig. S.1. The measurement strength  $\gamma = |\vec{b}|$  is given by the length of the Bloch vector, furthermore if  $b_0 = 0$  the POVM is unbiased.

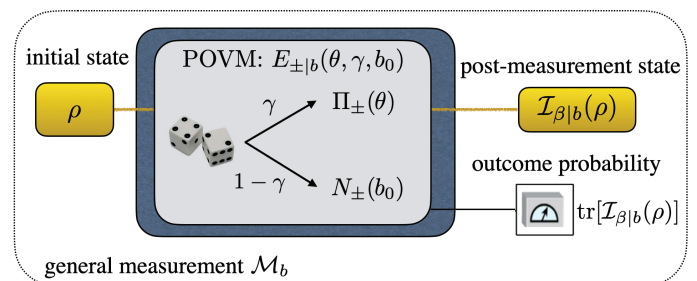


FIG. S.1. Schematic illustration of general measurement  $\mathcal{M}_a$  described by a set of positive operator-valued measures (POVMs)  $E_{\pm}(\theta, \gamma, b_0)$ . With probability  $\gamma$  a projective measurement  $\Pi_{\pm}(\theta)$  is carried out and with probability  $1 - \gamma$  a biased dummy measurement  $N_{\pm}(b_0)$ .

The unbiased POVM we study is given

$$E_{\pm|b}(\theta, \gamma, b_0 = 0) = (1-\gamma)\frac{\mathbb{1}}{2} + \gamma \underbrace{\frac{1}{2}(\mathbb{1} \pm \overbrace{\cos\theta\sigma_x + \sin\theta\sigma_z}^{\sigma_\theta})}_{\Pi_{\pm|b}(\theta)}, \quad (\text{S.2})$$

consisting of a projector  $\Pi_{\pm|b}(\theta)$  onto the eigenstates of  $\sigma_\theta$  with relative weight (probability)  $\gamma$ , and a contribution of a dummy measurement, as indicated by the unity operator in the POVM definitions from Eq. (S.2), with

weight  $1 - \gamma$ . In the actual experiment, the noisy POVM is realized by controlling the current in the respective coil (if  $\mathcal{M}_b$  is a POVM measurement that would be coil DC-4) with a random generator, switching with the given probabilities  $\gamma$  and  $1 - \gamma$  between the projective measurement and the dummy-measurement. In case of the projective measurement the direction  $\theta$  of the projector  $\Pi_{\pm}(\theta)$  is adjusted by the appropriate currents in the coil for the  $\pm$  direction. In the case of the dummy measurement, the current in the coil is switched off, resulting in random results for the no-measurement.

A biased POVM in its most compact form is denoted as

$$E_{\pm|b}(\theta, \gamma, b_0) = \frac{1}{2}((1 \pm b_0)\mathbb{1} \pm \gamma(\cos \theta \hat{\sigma}_x + \sin \theta \hat{\sigma}_z)), \quad (\text{S.3})$$

which for bias  $b_0 = 0$  reproduces Eq. (S.2). However, for the actual experimental implementation, it is useful to rewrite the POVM in the following form

$$E_{\pm|b}(\theta, \gamma, b'_0) = \gamma \Pi_{\pm}(\theta) + (1 - \gamma) N_{\pm}(b'_0) \quad (\text{S.4})$$

as a convex combination of projective measurement  $\Pi_{\pm}(\theta) = (\mathbb{1} \pm (\cos \theta \hat{\sigma}_x + \sin \theta \hat{\sigma}_z))/2$  and biased dummy (noisy) measurement  $N_{\pm}(b'_0) = (1 \pm b'_0)\mathbb{1}/2$ , which is fully characterized by three parameters, rotation angle  $\theta$  about a specific axes, bias  $b'_0 = b_0/(1 - \gamma)$ , and the randomization degree  $\gamma$ . Practically a voltage offset for the control of the current (and consequently the magnetic field) in the DC coils is used to create the biased behavior of the POVM.

### 3. Correlation and Disturbance

The successive measurement of  $\mathcal{M}_a$  and  $\mathcal{M}_b$  (sharp or unsharp) finally result in four recorded intensities denoted as  $I_{++}, I_{+-}, I_{-+}$ , and  $I_{--}$ , where the first index denotes the measurement orientation of the  $\mathcal{M}_a$  measurement and second for  $\mathcal{M}_b$ . Using these intensities the correlation  $\mathcal{C}$  is given by

$$\mathcal{C} = \frac{I_{++} + I_{--} - I_{+-} - I_{-+}}{I_{++} + I_{--} + I_{+-} + I_{-+}}. \quad (\text{S.5})$$

Furthermore, we can evaluate the disturbance  $\mathcal{D}$  as

$$\mathcal{D} = 2 \left| \frac{I'_+}{I'_+ + I'_-} - \frac{I_{++} + I_{-+}}{I_{++} + I_{--} + I_{+-} + I_{-+}} \right|, \quad (\text{S.6})$$

where  $I'_{\pm}$  accounts for the intensities obtained in a *target* measurement alone, that is a measurement with apparatus  $\mathcal{M}_a$  switched off, and therefore only two results are possible.

### 4. Search for optimal state

In case  $\mathcal{M}_a = \vec{a} \cdot \vec{\sigma} = \cos \theta \sigma_x + \sin \theta \sigma_z$  and  $\mathcal{M}_b = \vec{b} \cdot \vec{\sigma} = \sigma_x$  with associate Bloch vector  $\vec{a} = (\cos \theta, 0, \sin \theta)$

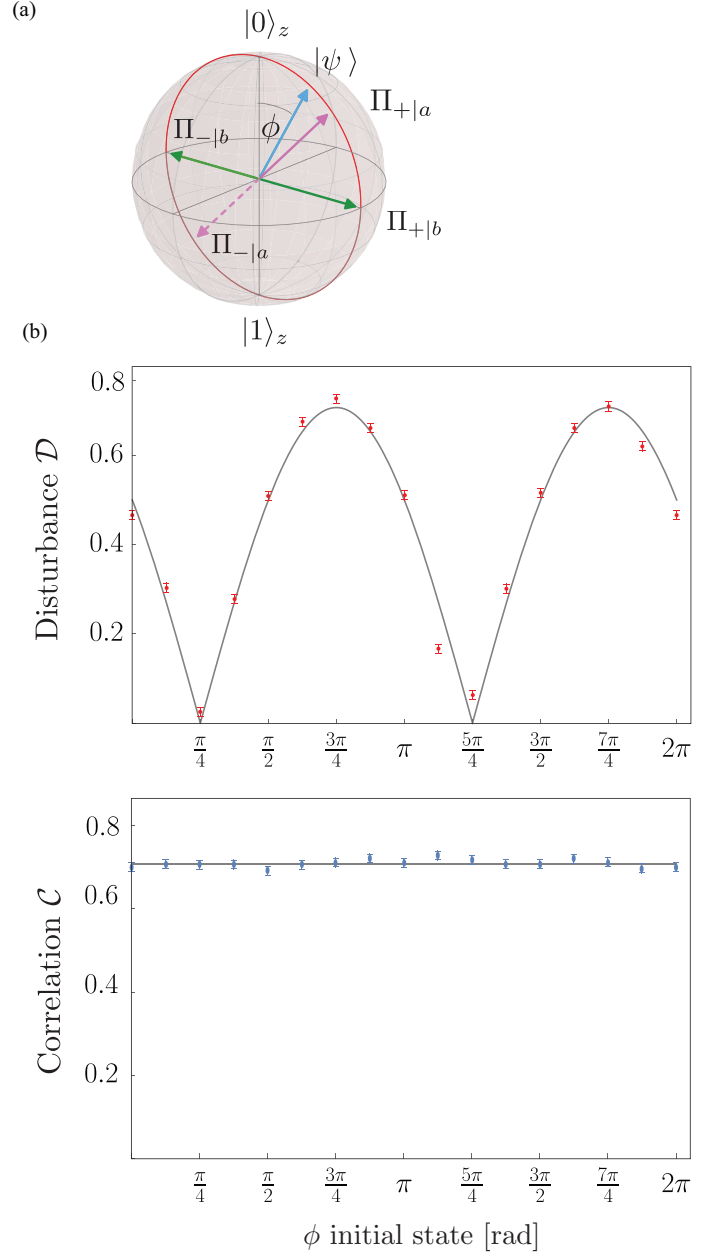


FIG. S.2. Experimental determination of optimal state  $|\psi_{\text{opt}}\rangle$  by varying the polar angle  $\phi$  of the initial state  $|\psi\rangle$ . (a) Bloch sphere description of  $\mathcal{M}_a$ ,  $\mathcal{M}_b$  and  $|\psi\rangle$ . (b) Correlation  $\mathcal{C}$  and disturbance  $\mathcal{D}$  versus polar angle  $\phi$  of the initial state  $|\psi\rangle$

and  $\vec{b} = (1, 0, 0)$ , the optimal state is the eigenstate of

$$\vec{a} \times (\vec{a} \times \vec{b}) \cdot \vec{\sigma} = (1 - \cos^2 \theta) \sigma_x - \cos \theta \sin \theta \sigma_z \quad (\text{S.7})$$

$$\vec{a} \times (\vec{a} \times \vec{b}) \cdot \vec{\sigma} = \sin^2 \theta \sigma_x - \cos \theta \sin \theta \sigma_z \quad (\text{S.8})$$

with eigenvector,

$$\frac{1}{2}(\mathbb{1} \pm \hat{n} \cdot \vec{\sigma}) \quad , \quad \hat{n} = (\sin^2 \theta, 0, -\cos \theta \sin \theta)/|\vec{n}| \quad (\text{S.9})$$

Here we present an experimental determination of the optimal state. The fore we fix the  $\mathcal{M}_a$  measurement at  $\theta = \pi/4$  resulting in  $\mathcal{M}_a = 1/\sqrt{2}\sigma_x + 1/\sqrt{2}\sigma_z$  and vary the polar angle  $\phi$  of the initial state  $|\psi\rangle$  between 0 and  $2\pi$ , which is depicted in Fig. S.2 (a). As seen in Fig. S.2 (b) the maximal disturbance  $\mathcal{D}$  is reached at  $\phi = 3\pi/4$  and  $\phi = 7\pi/4$ , that is when the initial state is orthogonal to the direction of the  $\mathcal{M}_a$ . In addition, we see the state-independence of the correlation  $\mathcal{C}$  resulting in a constant value  $\mathcal{C} = 1/\sqrt{2}$  for all settings of  $\phi$ .

### 5. Effect of POVM's post-measurement state

The main consequence is that now the *post-measurement* state of the POVM, denoted as  $\rho_{\text{out}}$  plays a crucial role, representing an additional experimental parameter. Three cases are investigated and the results can be seen in Fig. S.3: i) the post-measurement states of the POVM are the eigenstates of the projectors  $\rho_{\text{out}} = |\pm x\rangle$ , ii) mixed states with interaction strength  $\gamma$   $\rho'_{\text{out}} = 1/2(\mathbb{1} + \gamma\sigma_x)$ , and iii) decomposition using the underlying Kraus operators  $\rho''_{\text{out}} = K_{\pm|a}^\dagger \rho_{\text{in}} K_{\pm|a} / \text{Tr}(\hat{\Pi}_{\pm|a} \rho_{\text{in}})$ , with  $K_{\pm|a}^\dagger K_{\pm|a} = \hat{\Pi}_{\pm|a}$ , as required for the so-called Lüder instrument in the main text.

In the first case  $\rho_{\text{out}} = |\pm x\rangle$ , where the post-measurement states  $\rho_{\text{out}} = |\pm x\rangle$  equals that from a projective measurement (see Fig. S.3 (a) and (b)), the correlation-disturbance tradeoff relation equals one of two projective measurements, which is plotted in Fig. S.3 (c) red data points. The reason for this lies in the particular choice of the optimal initial state  $|\psi_{\text{in}}\rangle$ , which is perpendicular to the direction of the POVM elements  $E_{\pm|a}(\theta, \gamma, a_0)$ . Hence, the output probabilities are 1/2 for both results - the same as for a projective measurement. Since the post-measurement states  $\rho_{\text{out}} = |\pm x\rangle$  equals that from a projective measurement the correlation-disturbance tradeoff relations from projective measurements and POVM with post-measurement states  $\rho_{\text{out}} = |\pm x\rangle$  are indistinguishable.

In the second case, we study a mixed state  $\rho'_{\text{out}} = 1/2(\mathbb{1} + \gamma\sigma_x)$ , with interaction strength  $\gamma = 1/2$  as post-measurement state of the POVM. An interesting behavior is observed: for compatible measurement settings (see Fig. S.3 (a)), that is  $\theta = 0$  the correlation reproduces the interaction strength  $\mathcal{C}(\theta = 0) = 0.5 = \gamma = |\vec{a}|$  (see Fig. S.3 (c) blue data points), as in the case where the measurement order is reversed. However for maximally incompatible orientation of the measurement directions, that is  $\theta = \pi/2$  we get disturbance  $\mathcal{D} = 1$ , which is the same result as for both measurements being projective.

Finally, we have the third case, where the correspond-

ing post-measurement state, according to the transformation rule, is described by  $\rho \mapsto \mathcal{I}_{\alpha|a}(\rho) = K_{\alpha|a} \rho K_{\alpha|a}^\dagger$  with outcome probability  $p_{\alpha|a} = \text{tr}[\mathcal{I}_{\alpha|a}(\rho)]$  and  $E_{\alpha|a} = K_{\alpha|a}^\dagger K_{\alpha|a}$  as  $\rho''_{\text{out}} = K_{\pm|a}^\dagger \rho_{\text{in}} K_{\pm|a} / \text{Tr}(\hat{\Pi}_{\pm|a} \rho_{\text{in}})$ . Surprisingly the post-measurement state  $\rho''$  of the POVM

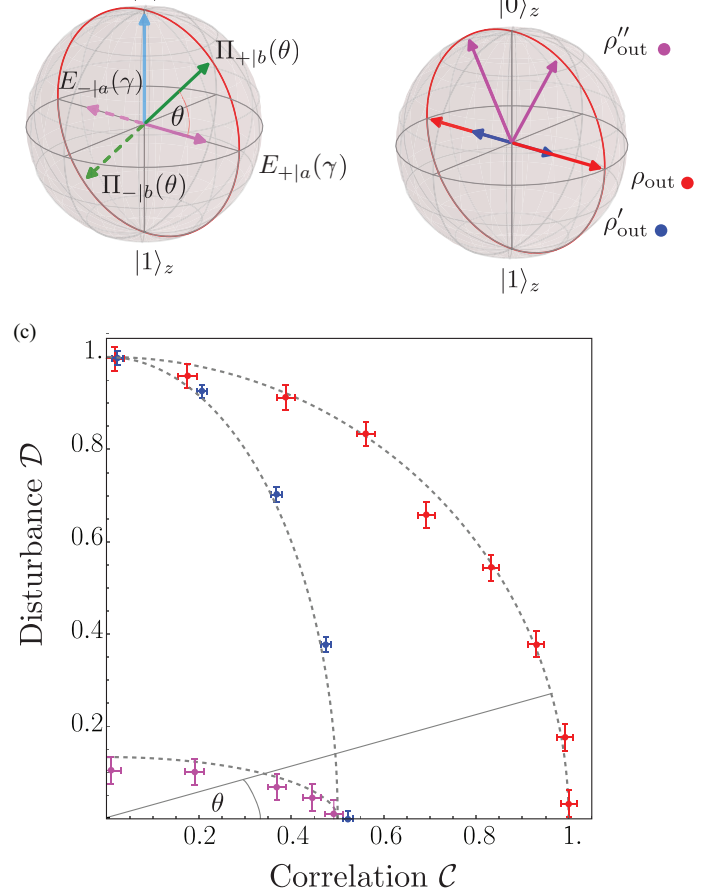


FIG. S.3. Effect of POVM's post-measurement state. (a) Bloch sphere representation of measurement settings (b) Bloch sphere representation for post-measurement states pure (red), mixed state (blue), and effect - or Lüder state- (purple). (c) Correlation-disturbance tradeoff for the three post-measurement states.

$E_{\pm|a}(\gamma)$  is a pure state, due to the particular choice of the optimal initial state  $|\psi\rangle$ . Here an important feature of an unsharp (or general) measurement becomes apparent: the unsharp measurement has less disturbance compared to a projective measurement. For  $\theta = \pi/2$  (maximally incompatible) the disturbance yields  $\mathcal{D} = 0.1$  (Fig. S.3 (c) purple data points), whereas in the case of a projective measurement, we have  $\mathcal{D} = 1$  in this case.